Lipid Diffusion from Single Molecules of a Labeled Protein Undergoing Dynamic Association with Giant Unilamellar Vesicles and Supported Bilayers

Alexey Sharonov,[†] Rakeshwar Bandichhor,[‡] Kevin Burgess,[‡] Anca D. Petrescu,[§] Friedhelm Schroeder,[§] Ann B. Kier,[||] and Robin M. Hochstrasser*,[†]

Department of Chemistry, University of Pennsylvania, Philadelphia, Pennsylvania 19104-6323, Department of Chemistry, Texas A&M University, Box 30012, College Station, Texas 77841, and Departments of Physiology & Pharmacology and Pathobiology, Texas A&M University, TVMC, College Station, Texas 77843-4467

Received June 20, 2007. In Final Form: October 31, 2007

It is demonstrated that single-molecule tracking of a fluorescently labeled protein undergoing transient binding to model membranes presents a useful method of obtaining fluid properties. The labeled ACBP protein was tracked during its binding to free-standing giant unilamellar vesicles (GUVs) and supported bilayers prepared from the GUVs in the same environment. The analysis of images that are blurred as a result of fast probe diffusion was discussed. An examination of the lateral diffusion trajectories revealed a homogeneous diffusion on the top segments of the GUVs with $D = 6.9 \pm 0.3$ μm^2/s. The supported bilayer experiments revealed two diffusion processes, one with $D_f = 3.1 \pm 0.4$ μm^2/s and the other with $D_s = 0.078 \pm 0.001$ μm^2/s. The 2-fold difference in the lipid bilayer mobility for the free-standing and fast components in the supported bilayers is attributed to the known effect of frictional coupling with the solid support. The slow mobile fraction in the bilayer is suggested to be associated with the migration of pore-like structures, originating from the interaction of the membrane with the glass support.

Introduction

The biological activity of cells depends on the properties of the cell plasma membrane. Although the lipid bilayer is the main component of the membrane, the lateral mobility of the membrane's components is not uniform and can be very complex because of multiple interactions with proteins and cell cytoskeleton. Descriptions of the local inhomogenietites of the membrane as mosaics[1] and lipid rafts[2] have become a focus of studies of heterogeneous biological membranes. Single-particle tracking (SPT) experiments permit observations of individual probes in sub-micrometer domains. It is common to use either fluorescently labeled lipids or attached gold nanoparticles as probes for tracking,[3] both of which require special preparation and incorporation of labels into the membranes. In the present paper, we propose an approach of testing the bilayer properties by means of fluorescent probes dynamically associated with lipids. The probes are freely diffusing in the surrounding solution and spontaneously binding to lipids of the bilayer. They then migrate with the lipids with a mobility that depends on properties of the bilayer. In this approach there is an infinite reservoir of non-photobleached fluorescent probes. The method does not require incorporation of probes into the bilayer[4−10] or their attachment to lipid via an appropriate linker,[11] and it is amenable to applications in live cell plasma membranes. To verify the approach we focused on SPT measurements where a fluorescently labeled acyl-CoA binding protein (ACBP)[12,13] acts as the probe of bilayer fluidity in liquid-phase phospholipid bilayers (SPB) and giant unilamellar vesicles (GUV).

Even for a single-phase bilayer, lipid mobilities in supported and free-standing bilayers vary depending on the type of membrane. This conclusion is based on fluorescence recovery after photobleaching (FRAP) and fluorescence correlation spectroscopy (FCS) measurements. Coefficients of diffusion in a GUV fluid bilayer are in the range of 3−8 μm^2/s[5,8,14−17] and they depend on the lipid composition, temperature and properties of the surrounding solution. The mobility of lipids in SPB is not only influenced by interactions with the support[4−6,18−20] but is also sensitive to properties of the bilayer endowed by its method of preparation[9] such as Langmuir−

* To whom correspondence should be addressed. E-mail: hochstra@sas.upenn.edu. Phone: 215-898-8410. Fax: 215-898-0590.
[†] University of Pennsylvania.
[‡] Department of Chemistry, Texas A&M University.
[§] Departments of Physiology & Pharmacology, Texas A&M University.
[||] Department of Pathobiology, Texas A&M University.

(1) Singer, S. J.; Nicolson, G. L. *Science* **1972**, *175*, 720−731.
(2) Simons, K.; Meers, G. V. *Biochemistry* **1988**, *27*, 6197−6202.
(3) Fujiwara, T.; Ritchie, K.; Murakoshi, H.; Jacobson, K.; Kusumi, A. *J. Cell Biol.* **2002**, *157*, 1071−1081.
(4) Schutz, G. J.; Schindler, H.; Schmidt, T. *Biophys. J.* **1997**, *73*, 1073−1080.
(5) Przybylo, M.; Sykora, J.; Humpoliekova, J.; Benda, A.; Zan, A.; Hof, M. *Langmuir* **2006**, *22*, 9096−9099.
(6) Sonnleitner, A.; Schutz, G. J.; Schmidt, T. *Biophys. J.* **1999**, *77*, 2638−2642.
(7) Ladha, S.; Mackie, A. R.; Harvey, L. J.; Clark, D. C.; Lea, E. J. A.; Brullemans, M.; Duclohier, H. *Biophys. J.* **1996**, *71*, 1364−1373.
(8) Schwille, P.; Korlach, J.; Webb, W. W. *Cytometry* **1999**, *36*, 176−182.
(9) Starr, T. E.; Thompson, N. L. *Langmuir* **2000**, *16*, 10301−10308.
(10) Schmidt, T.; Schutz, G. J.; Baumgarner, W.; Gruber, H. J.; Schindler, H. *Proc. Natl. Acad. Sci. U.S.A.* **1996**, *93*, 2926−2929.
(11) Yoshina-Ishii, C.; Chan, Y.-H. M.; Johnson, J. M.; Kung, L. A.; Lenz, P.; Boxer, S. G. *Langmuir* **2006**, *22*, 5682−5689.
(12) Kragelund, B. B.; J, K.; F. M., P. *Biochim. Biophys. Acta* **1999**, *1441*, 150−161.
(13) Chao, H.; Martin, G. G.; Russell, W. K.; Waghela, S. D.; Russell, D. H.; Schroeder, F.; Kier, A. B. *Biochemistry* **2002**, *41*, 10540−10553.
(14) Kahya, N.; Schwille, P. *Mol. Membr. Biol.* **2006**, *23*, 29−39.
(15) Kahya, N.; Scherfeld, D.; Bacia, K.; Poolman, B.; Schwille, P. *J. Biol. Chem.* **2003**, *278*, 28109−28115.
(16) Bacia, K.; Schwille, P.; Kurzchalia, E. *Proc. Natl. Acad. Sci. U.S.A.* **2005**, *102*, 3272−3277.
(17) Korlach, J.; Schwille, P.; Webb, W. W.; Feigenson, G. W. *Proc. Natl. Acad. Sci. U.S.A.* **1999**, *96*, 8461−8466.
(18) Zhang, L.; Granick, S. *Proc. Natl. Acad. Sci. U.S.A.* **2005**, *102*, 9118−9121.
(19) Wagner, M. L.; Tamm, L. K. *Biophys. J.* **2000**, *79*, 1400−1414.
(20) Seu, K. J.; Pandey, A. P.; Haque, F.; Proctor, E. A.; Ribbe, A. E.; Hovis, J. S. *Biophys. J.* **2007**, *92*, 2445−2450.

10.1021/la702600w CCC: $40.75
Published on Web 01/09/2008

Blodgett deposition[4,6] or adsorption/fusion of lipid vesicles.[21,22] It has been shown recently that when the conditions are identical the mobility in free-standing bilayers is significantly higher than in the supported ones.[5]

Although FRAP and FCS measurements give precise measures of average diffusion, it can be challenging to detect deviations from Brownian motion in such experiments. The diffusion of lipids in the bilayer can be influenced by local inhomogenieties and/or the interactions with the support. For example, SPT experiments[4,6] have revealed the coexistence of two diffusion processes in a single liquid phase supported bilayer whereas in most FRAP and FCS measurements the slower of the two mobile fractions is not evident.

We compared fluid properties of GUV free-standing bilayers and bilayers obtained by rupturing the GUV, which allowed direct comparisons of the results. Our particular interest was in tracking the fluorescent probe on the GUV surface. The previously reported permeability of GUV membranes[23,24] could be initiated by the existence of defects on the GUV surface, which would be detectable in the tracking experiments. To the best of our knowledge there were no previous studies where single-molecule tracking was performed on the surface of giant vesicles. The diffusion in free-standing planar membranes (black membranes) was found to be 4−5 times faster than for Langmuir−Blodgett supported bilayers and did not contain any slow mobile fraction.[6] However the methods of preparation of these bilayers were different and there remain interesting questions as to whether the slow-mobile fraction originates from interactions with the solid support or is associated with defects or impurities in the bilayer.

An entirely new approach to measuring diffusion in membranes by using dynamically bound protein is introduced in this work. The first study of diffusion in GUVs using methods that are not ensemble averaged are reported. Tracking of a single ACBP protein on the surface of a giant vesicle evidence homogeneous Brownian type diffusion with a single diffusion constant. The diffusion in the supported bilayer is found to have both a fast and a slow components, where the slow moving fraction is not determined by composition or impurity but by the defects that are created by interaction with the glass. The binding affinity for the probe at the slow moving sites is demonstrably different from the bulk proving that the membrane configurations are disturbed. The slow fraction is suggested to arise from pore-like defects.

Materials and Methods

Materials. Lipid (POPC, 16:0−18:1 PC 1-palmitoyl-2-oleoyl-*sn*-glycero-3-phosphocholine) was purchased from Avanti Polar Lipids; Hepes buffer, sodium chloride and sucrose were from Fisher Chemical and chloroform was from Acros Organics. D-(+) Glucose was from Sigma. Glass coverslips and cylinders (Fisher) were cleaned by sonication for 1 h in Piranha Solution (3:1 mixture of sulfuric acid and 30% hydrogen peroxide) with sequential extensive washing in UltraPure water (Millipore Corporation).

ACBP Purification and Labeling. Recombinant mouse ACBP[13] (10 KDa) was histidine-tagged by subcloning into pET21B plasmid (from Novagen, EMD Chemicals Inc., San Diego, CA) and expressed in *E. coli* BL21. Histidine-tagged ACBP was further purified from bacterial cell lysate by affinity chromatography on Ni-CAM resin from Sigma-Aldrich (St.-Louis, MO). A water-soluble rhodamine-based dye synthesized as described[25] was used to chemically label purified ACBP. A dye-to-protein molar ratio of 5:1 was found to be optimal for dye/protein incubation at room temperature for 1 h in phosphate buffer saline (PBS), pH 8.5 in order to couple an average of one fluorophore per ACBP molecule. The rhodamine-ACBP conjugate was isolated from unbound dye by gelfiltration on a 20 mL Bio-Gel P-4 (Bio-Rad Laboratories, Hercules, CA) column equilibrated in PBS, pH 7.4. Rhodamine-labeled ACBP was characterized in terms of structural and functional properties as previously described[25] and was demonstrated to maintain its secondary structure and affinity for fluorescent acyl-coenzyme A's such as *cis*-parinaroyl-CoA.

Sample Preparation. The GUVs were prepared by electroformation.[26] Briefly, 10 μL of 0.2 mg/mL lipid solution in chloroform was deposited on indium tin oxide (ITO) coated glass and subsequently dried by a nitrogen flow and in vacuum for 1 h. The GUVs were grown in an electric field applied between two ITO coated glass plates separated by a 2 mm rubber spacer. A 10 Hz sinusoidal voltage was applied to the electrodes at 0.5 V/mm while the chamber was filled with 0.2 M sucrose solution. The electric field was gradually raised up to 1.5 V/mm in steps of 0.1 V, applied every 5 min by means of a function generator, based on an NI-DAC board (National Instruments). The growth of the vesicles was visually monitored by differential interference contrast (DIC) microscopy. Vesicle formation was continued for 1 h at 1.5 V/mm. The GUVs were then gently removed by a syringe and stored at 4 °C.

The GUV suspension (1 μL) was added to a 100 μL chamber (cell separation glass cylinder located on a microscope glass slide). The chamber was filled with a 100 mM NaCl 10 mM Hepes (pH 7.4) buffer having close to GUVs interior osmolarity. The GUV sank to the bottom of the glass vessel and either attached to the surface or spontaneously ruptured. The mean diameter of GUVs prepared in this manner was in the range of 10−20 μm. Ruptured GUVs form isolated supported bilayers on the glass surface with exactly same composition as the parent GUV. These supported bilayers and the non-ruptured GUVs were used in the tracking experiments in order that two types of membranes in the same environments could be compared.

Microscopy. The methods are based on a commercial Olympus IX81 inverted microscope. The laser beams from Kr^+ (568 nm) ion laser pass through a quarter-wave plate to generate circularly polarized light, expansion optics, mechanical PC controlled shutter and appropriate lenses to focus the excitation onto the back focal plane of an oil-immersion objective (Olympus 60× NA = 1.45). A lens, coupled with a translation stage, was used to align the excitation beam across the objective's back aperture to achieve easy illumination, angle adjustment, and interconversion of the setup between through-the-objective TIR and epi-fluorescence microscopy. The excitation light was filtered by appropriate laser band-pass filters and dichroic mirrors (Chroma). Fluorescence from the sample was collected by the objective and directed to a CCD camera with multiplication-on-chip capability (Roper Scientific, Cascade 512F) by means of a beam splitter and an appropriate set of band-pass filters (Omega Optical). With the 1.6× lens the total magnification of the microscope was 96×, which yields a pixel size in the image plane of the camera of ∼167 nm. Time-lapsed image recording and control of the microscope was performed by especially designed LabView (National Instruments) based software. The recorded sequences of frames were analyzed by in-house developed software based on MATLAB (The MathWorks Inc.). All experiments were conducted at room temperature at ∼50 frames/s. A CW excitation laser beam provided a power of 1 kW/cm^2 in the sample plane. Typically, 300−500 frames were collected in each measurement.

Tracking in supported lipid bilayers was performed in the total internal reflection (TIR) geometry.[27] For imaging of optical cross sections of GUVs the excitation beam was directed at a low angle

(21) Barenholz, Y.; Gibbes, D.; Litman, B. J.; Goll, J.; T. E. Thompson, D.; Carlson, F. *Biochemistry* **1977**, *16*, 2806−2810.
(22) Brian, A. A.; Mcconnell, H. M. *Proc. Natl. Acad. Sci. U.S.A.* **1984**, *81*, 6159−6163.
(23) Estes, D. J.; Mayer, M. *Biochim. Biophys. Acta* **2005**, *1712*, 152−160.
(24) Fischer, A.; Oberholzer, T.; Luisi, P. L. *Biochim. Biophys. Acta* **2000**, *1467*, 177−188.
(25) Rakeshwar, B.; Petrescu, A. D.; Vespa, A.; Kier, A. B.; Friedhelm, S.; Burgess, K. *Bioconjugate Chem.* **2006**, *17*, 1219−1225.
(26) Angelova, M. I.; Dimitrov, D. S. *Prog. Colloid Polym. Sci.* **1988**, *76*, 59−67.
(27) Axelrod, D. *Methods Cell Biol.* **1989**, *30*, 245−70.

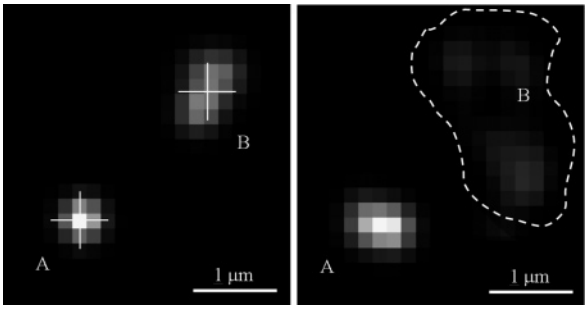

Figure 1. Simulated images of diffusing fluorophores (see text for details). A and B are images of two fluorophores with lateral diffusion coefficients of 0.1 μm^2/s and 5 μm^2/s. Left panel: 20 ms exposure time. Right panel: 200 ms exposure time. The blured image of fluorophore B in the right panel is highlighted by dashed line. The crosses show locations of fluorophores obtained from the weighted average.

to the interface. In this low-angle epi-illumination (or grazing angle) configuration[28] relatively thin layers (typically 7−10 μm thickness) are illuminated, thus reducing the background signal from fluorescent molecules in the solution compared with the conventional epi-illumination scheme. The vertical resolution of the microscope depends on the focus depth of the objective (1−1.5 μm in our case) so only molecules localized in 1−1.5 μm thick cross section appear as diffraction limited spots. The low background from this approach allows visualization of temporally immobilized single molecules at some distance from the interface even in fluorescent solutions.

Single-Molecule Tracking. We analyzed the diffusion by tracking the trajectory of the individual fluorophore position, $r(t) = (x(t), y(t))$, over time.[29,30] The analysis of the images and the tracking was performed in several stages. In the first stage each image in a sequence was passed through a 2D cutoff digital filter in order to reduce the high-frequency noise of the CCD detector. The recognition of fluorescent spots was performed by the software automatically by means of a threshold, finding contours of equal intensity for each spot and determination of the mean X and Y values of the contour. Since the mean square displacement (MSD) of 2D Brownian motion is proportional to $4Dt$, the exposure time becomes important for relatively fast motion. Indeed, the diffusion of a single lipid in a lipid bilayer with $D \approx 3-5$ μm^2/s implies a high probability for this lipid to explore an area of 0.24−0.4 μm^2 area during a 20 ms exposure: this area significantly exceeds the size of a pixel. The light pattern from such a single fluorophore is non-symmetrical and cannot be fitted with the point spread function (PSF) to determine its spot location.

Figure 1 shows simulated images of a diffusing fluorophore. The image was obtained by using a Gaussian PSF with $\sigma_x = \sigma_y = 0.148$ μm. The mean value of the PSF was computed at the end of each segment consisting of a 100 step Brownian trace. The diffusion coefficients were set to be 0.1 μm^2/s (spot A) and 5 μm^2/s (spot B), the total time of the trace was 20 ms (0.2 ms/point) in the left panel and 200 ms (2ms/point) in the right panel of the figure. The spot A can be considered as immobile during 20 ms exposures, its shape is close to a diffraction limited Gaussian distribution. The spot B is one of the expected shapes if the fluorescent spot is moving during the 20 ms exposure frame. The shape is no longer defined by the diffraction limit but is extended and asymmetrical. Information regarding the diffusion coefficient can be visualized from single-molecule spot size analysis.[31]

The precise location of a diffusing fluorophore cannot be determined by means of the common procedure of Gaussian fitting. We define the location of such extended spots as a weighted average of positions of all pixels forming the spot's image. The more time the fluorophore spends in the pixel area the brighter is the pixel, thus the mean location of the molecule during the exposure time can be calculated as

$$\bar{s} = \frac{\sum_{i=1}^{N} a_i s_i}{\sum_{i=1}^{N} a_i} \quad (1)$$

where a_i is the intensity and s_i represents the x, y coordinates of the ith of N pixels in the single spot image. The average locations of fluorescent spots determined by this method are marked as crosses in Figure 1. If two fluorophores emit the same number of photons, the one moving faster has smaller intensity because of the averaging. The difference in intensities between spots serves as a selection for two differently diffusing fractions of molecules as shown in Figure 1 (right). If the diffusion coefficients differ significantly, the fraction of fast moving molecules can be excluded by a choice of the threshold.

Trajectories were reconstructed from the coordinates of each spot by motion analysis software (Matlab). In the first pass every molecule was tracked by finding its coordinates in neighboring time frames. The diffusion coefficient was introduced into the program as a parameter to find the most probable location of the molecule. In our experiments the fluorescent probe may bind to the membrane spontaneously at any instant, thereby initiating a new trajectory, which is recognized by the software. In the second pass of the program, possible conflicts where the same molecule appears in two trajectories were reanalyzed. We also excluded from analysis all trajectories showing very unusual behavior such as those with large changes in multiple sequential steps, indicating a changing in the mode of motion during the trajectory. Finally, each trajectory in the recorded movie was verified visually to eliminate those that include two molecules whose paths cross or any other complications.[32] In several cases when molecular motion creates significant blurring or several molecules are within close proximity, the software cannot correctly recognize the trajectory. In such cases we manually located the approximate positions of the fluorescent spots, the exact position was then adjusted by the software algorithms described above.

The mean-square displacement was calculated from the individual trajectories by internal averaging of all pairs of points[29,30] in a trajectory. Although the average over all pairs instead over all independent pairs does not improve the signal-to-noise ratio much because of the high correlation of the overlapping pairs, at large time separation the averages over all pairs are smoother.[30] The survival time of the fluorophore is limited by single step photobleaching, thus limiting the range of molecular motion. The standard deviation σ of the distribution is described by σ[29]

$$\sigma = D\left[\frac{2N_D}{3(N_T - N_D)}\right]^{1/2} \quad (2)$$

where D is a diffusion coefficient, N_T is the total number of positions measured in the trajectory and N_D is the number of steps used to calculate the least-square fit. In our experiments N_D was set at 5. N_T was varied in a range of 10−50 depending on the experiment. We performed random-walk simulations with parameters close to the experimental ones ($t_{exp} = 20$ ms, $T = 20$ms, $N_T = 20$, $N_D = 5$, $D = 3$ μm^2/s) and 500 traces at a resolution of 0.2 ms/step were analyzed. The distribution of the diffusion coefficients (Figure 2, dotted line) is close to expectations from eq 2. The same trajectories were analyzed by simulating the spot location at every time point, as described above. Then the locations of spots in the simulation were determined by the same averaging procedure as used in the experiments. The distribution obtained in this manner (Figure 2, solid line) was very close to the distribution obtained from the known exact position of the molecule (Figure 2, dotted line). Although the exact position of the molecule in the middle of a 20 ms interval is

(28) Sharonov, A.; Hochstrasser, R. M. *Biochemistry* **2007**, *46*, 7963−7972.
(29) Qian, H.; Sheetz, M. P.; Elson, E. L. *Biophys. J.* **1991**, *60*, 910−921.
(30) Saxton, M. J. *Biophys. J.* **1997**, *72*, 1744−1753.
(31) Schuster, J.; Cichos, F.; Borczyskowski, C. V. *J. Phys. Chem. A* **2002**, *106*, 5403−5406.
(32) Anthony, S.; Zhang, L.; Granick, S. *Langmuir* **2006**, *22*, 5266−5272.

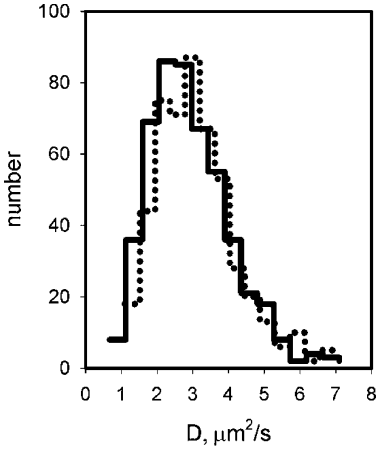

Figure 2. Simulated distribution of diffusion coefficients ($D = 3$ μm^2/s). Histograms represent the distribution of diffusion coefficients calculated by analyzing of 20 steps-long trajectories. The exact locations of the fluorophore (dotted line) and those determined by the image analysis procedure (solid line) are shown (see text for details).

not known, the averaged position determined by the weighted mean procedure gives very close to the correct diffusion coefficient.

The averaged diffusion coefficients were determined from MSD vs time plots. Mean square displacements were first obtained from all steps in all trajectories yielding the averaged values with their appropriate standard deviations: the latter were then used in further, weighted linear least-squares fits of the MSD time dependence and the quoted error in the diffusion constant corresponds to the standard error of this fit.

Results

Association of ACBP to Neutral Membranes. In a previous publication it has been demonstrated by methods of steady-state fluorescence and circular dichroism spectroscopy that ACBP binds to anionic phospholipid membranes[13] and that a negative surface charge and a high surface curvature of the membrane are important for ACBP association. We have examined the association of ACBP with model membranes by direct imaging methods at the single-molecule level. ACBP collisional flux was balanced against the photobleaching rate by adjusting the concentration of the protein (3.6×10^{-8} M) to maintain significant spatial separations between molecules on the bilayer surface.[33] We found that the ACBP not only binds to anionic phospholipids but also associates with neutral membranes at physiologically important ionic strengths. The molecular mechanism of association with neutral membranes has not yet been determined but the interaction may be promoted by insertion of aromatic residues into the lipid core.[34]

The image of fluorescently labeled ACBP bound to the POPC supported bilayer shown in Figure 3a corresponds to an exposure time of 20 ms. Each single fluorophore attached to the bilayer surface appears as a bright dot in the image. The molecules bound to the lipids are migrating along the surface of the bilayer (see also Movie 1 in Supporting Information). Figure 3b is a result of averaging of 50 frames. The bright spots outside the round bilayer patch are ACBP proteins that are immobilized on the glass surface, while the entire surface of the bilayer patch appears gray because of the motion of the membrane bound labeled proteins. The slowly diffusing fraction of molecules show up as bright spots in the center of the bilayer area in Figure 3b:

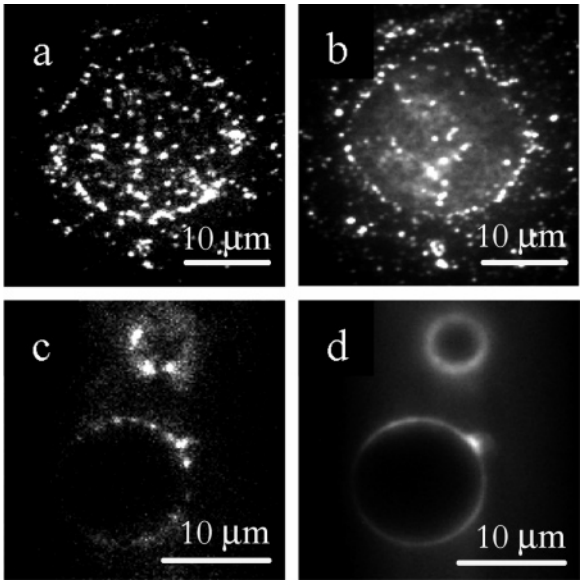

Figure 3. Images of fluorescently labeled ACBP bound to (a, b) a supported membrane and (c, d) a region shown as an equatorial cross section of a GUV. Both a and c are single 20 ms frames while b and d are the results of averaging 50 frames.

their motion is not blurred by averaging. The bright contour around the edges of the bilayer in Figure 3a,b indicated that the protein has a higher binding affinity to these regions. This result is likely to be caused by curvature: the association is more efficient when the close packing of the lipids is interrupted and the lipid hydrophobic core is more accessible.[13] Figure 3c,d shows the equatorial cross sections of two POPC GUVs. The ACBP binds similarly to the freestanding and supported bilayers. However, in the average image (Figure 3d) of the GUVs there are no sharp spots corresponding to slowly diffusing molecules. The GUV surface is uniformly bright. The small bright spot in the right upper part of the larger GUV is not a single fluorophore but it originates from a small vesicle coincidentally attached to the surface.

Diffusion of ACBP on the Surface of GUVs. The membrane segments at the top of GUVs were used to track proteins whose motion would be influenced by the glass interface. The GUVs selected for tracking had diameters exceeding 30 μm. The focus depth is $\sim$1$-$1.5 μm, thus the projection of the top segment is a disk with a diameter of ca. 15 μm. Over 30 trajectories on three different GUVs were selected by using the criterion that at least 12 sequential steps occurred. Although the proteins are moving along a curved membrane, the error in positioning is quite small when planarity is assumed in the calculation of the mean square displacements. The distribution of diffusion constants obtained for each individual trajectory displayed in Figure 4a has a mean value $D = 6.7$ μm^2/s with $\sigma = 2.4$ μm^2/s. The large σ arises from the lengths of the trajectories[29,30] which are limited by photobleaching and by proteins leaving the observation area. Furthermore, at the 20 ms exposure the blurring caused by the fast motion could have caused some spots to fall below the threshold criteria. The time dependence of the MSDs averaged over all steps in all trajectories is shown in Figure 4b. Although errors in the MSDs become larger at longer times (gray bars in Figure 4b) the data show an excellent linear time dependence indicating a diffusion coefficient $D = 6.9 \pm 0.3$ μm^2/s. There was no slow diffusing fraction in this case.

Diffusion of ACBP in a Supported Bilayer. The diffusion of ACBP bound to a supported bilayer was found to be remarkably different from the diffusion on the GUV surface. The diffusion

(33) Sharonov, A.; Hochstrasser, R. M. *Proc. Natl. Acad. Sci. U.S.A.* **2006**, *103*, 18911−18916.
(34) Wimley, W. C.; White, S. H. *Nat. Struct. Biol.* **1996**, *3*, 842−848.

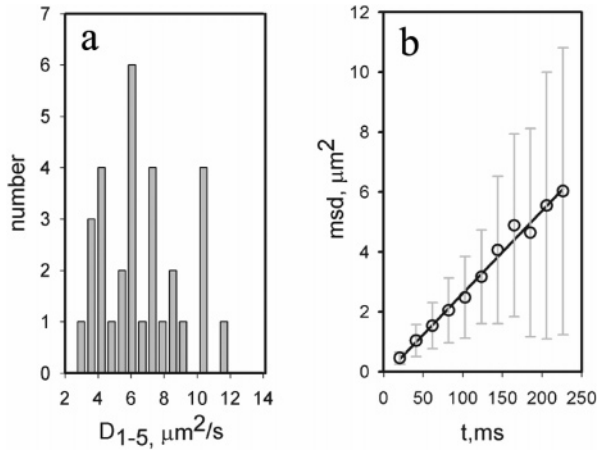

Figure 4. Diffusion coefficients of ACBP on a GUV surface. (a) Distribution of short-range diffusion coefficients obtained for individual trajectories. This distribution has a mean value $D = 6.7$ μm^2/s with a standard deviation of $\sigma = 2.4$ μm^2/s. (b) Time dependence of the mean square displacements (msd) averaged over all trajectories and time intervals. The solid line represents a fit yielding $D = 6.9 \pm 0.3$ μm^2/s; the gray bars are standard deviations.

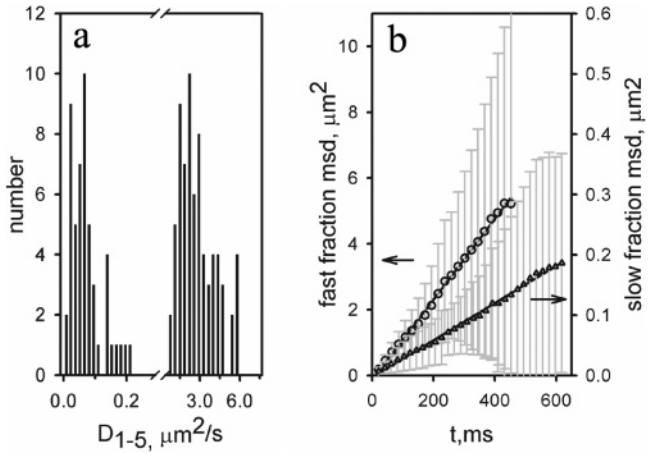

Figure 5. Diffusion coefficients of ACBP on a POPC supported bilayer. (a) Distribution of short-range diffusion coefficients obtained for individual trajectories. Histograms are shown for two coexisting fractions: fast (right); and slow (left). Mean values and standard deviations were $D_f = 2.8 \pm 1.3$ μm^2/s and $D_s = 0.07 \pm 0.05$ μm^2/s. (b) Time dependence of the mean square displacements (msd) averaged over all trajectories and time intervals. The solid line represents a fit yielding $D_f = 3.1 \pm 0.4$ μm^2/s (fast fraction, circles) and $D_s = 0.078 \pm 0.001$ μm^2/s (slow fraction, triangles), the gray bars are standard deviations.

was slower, and there were two coexisting fractions, one diffusing much faster then the other (see Movie 1 in Supporting Information). We applied a running-average procedure to the recorded sequence of frames. In this procedure each N frame in a sequence was averaged over neighboring frames as follows

$$I_j(x, y) = \frac{1}{n+1} \sum_{i=j-n/2}^{j+n/2} I_i(x, y), j = \frac{n}{2} \ldots N - \frac{n}{2}$$

where $I(x, y)$ is a 2D matrix of pixel intensities representing an image frame. The averaging window was selected to be $n = 10$ (200 ms), in order to allow discrimination of the slow and fast fractions by means of a threshold value as explained above (see Figure 1 right panel and Movie 2 in Supporting Information). The diffusion trajectories were obtained separately for the slow and fast fractions. We selected trajectories from at least 25 time steps for the fast molecules and 35 for the slow ones. The distribution of diffusion constants for individual trajectories are displayed in Figure 5a. Many of the fast moving protein tracks were discarded and not included in Figure 5 because they were not observed for a sufficiently long time even though it was clear they belonged with fast fraction. Therefore the ratio of the fast to the slow is underestimated by inspecting Figure 5. Approximately 5% of the total number of observed probe molecules were associated with the slow fraction. The distribution widths are close to those expected from eq 2. The mean fast (f) and slow (s) diffusion coefficients were $D_f = 2.8 \pm 1.3$ μm^2/s and $D_s = 0.07 \pm 0.05$ μm^2/s. In spite of the high variance in D the two distributions are clearly separated. The diffusion for each fraction was purely Brownian, as shown in Figure 5b, where the mean square displacement is plotted versus time for the first 20 (circles, fast fraction) and 30 (triangles, slow fraction) time steps. This manner of fitting gave $D_f = 3.1 \pm 0.4$ μm^2/s and $D_s = 0.078 \pm 0.001$ μm^2/s. No transitions between the fast and slow states of motion were observed within any single trajectory. In a few instances we detected trapping of the fast moving molecule into an ultraslow mode of motion. An example of this rare trapping process is displayed in Figure 6 (see also Movie 3 in Supporting Information) where a molecule undergoing the fast motion (83 steps of 20 ms each, gray line) is suddenly trapped to a slow mode of motion (black line) until it photobleached.

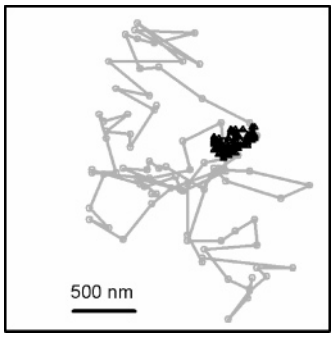

Figure 6. Example of a trapping event. The ACBP molecule diffusing in a POPC supported bilayer (the gray line represents 83 steps of 20 ms each) is suddenly trapped and becomes a slow mode (black line) where it remains until photobleaching. Both the fast and slow modes of motion are Brownian but the diffusion constants differ by more than a factor of 40 (see text).

Discussion

By harnessing the spontaneous collisions and subsequent binding of probes to lipid membranes we have provided a relatively direct and simple approach for testing bilayer mobility. No advance modification of the membrane is required, an advantage that could be enable applications to the visualization of live cell plasma membranes.

We found that the ACBP protein binds to neutral phospholipid bilayers for times that exceed the average photobleaching time of the fluorophore. The mechanism of binding is not yet known. We favor the idea that there are several of its aromatic residues anchored to the lipids as opposed to the water soluble ACBP becoming fully incorporated into the membrane. Neither the fraction of the protein volume that is inserted into the membrane nor the number of lipids bound to the protein are known. An issue that needs to be considered is the influence of the probe on the membrane properties, such as was observed for gold nanoparticles.[35] The hydrodynamic model[36] predicts a weak dependence of the coefficient of lateral diffusion with on the

(35) Lee, G. M.; Ishihara, A.; Jacobson, K. A. *Proc. Natl. Acad. Sci. U.S.A.* **1991**, *88*, 6274−6278.

embedded particle radius, however in a number of experiments deviations from this model were detected.[37−40] If the anchoring of the external label to the membrane involves multiple lipids, the diffusion may be retarded.

Notwithstanding the possibilities raised in the previous paragraph, the diffusion determined by tracking ACBP on the POPC GUV surface, $D = 6.9 \pm 0.3\ \mu m^2/s$, is very similar to expectations for diffusion of a single lipid in a liquid-disordered phase GUV membrane.[5,15,16,41] This comparison suggests that the present method is a viable approach not only for detection of local inhomogenieties but has potential for the determination of lateral diffusion constants.

The diffusion in a supported bilayer is usually slowed down because of interaction of the bilayer with the support. Although diffusion coefficients in GUVs and SPBs have been determined by various techniques,[5,6,9,15,16,19,41] direct comparison is difficult because of variations caused by many factors such as the reproducing the precise chemical environment, the methods of labeling and the variations in methods of preparation of supported bilayers. In one systematic study of GUVs and supported bilayers in very similar environments, a 2-fold difference in their diffusion coefficients was revealed.[5] It has also been shown that bilayers of similar composition, but obtained by different preparation techniques (Langmuir−Blodgett versus vesicle fusion) show differences in their diffusion properties.[9] The diffusion is known to be influenced by the support material and by the surface treatment.[9,20] Whether the monolayer−monolayer coupling is rather weak compared with the monolayer-substrate coupling[42] or whether the inner and outer leaflets of the bilayer are affected in the same way by interaction with the substrate[5,18] are not fully answered questions. The unwanted interaction of the label with the substrate[5,6] might be avoided by the use of labeled proteins because they may bind only to the outer leaflet of both membranes. The use of a properly designed external label could allow its interaction with the substrate to be avoided. Although we do not know how ACBP interacts with the lipids in the membrane, if the probe-membrane interaction involves only the headgroup region, the effect of the support on diffusion should be minimized.

In our comparison the GUV and SPB membranes were in precisely the same environment and their fluid properties were investigated by the same techniques. The supported membranes were obtained by rupturing the free-standing GUVs so that exactly the same composition and initial organization of lipids occurred for both, which were then investigated concomitantly in the same sample chamber. Although there were significant differences in preparation and detection methods compared with previous work, the diffusion coefficients in GUVs ($D = 6.9 \pm 0.3\ \mu m^2/s$) and supported bilayers (fast fraction, $D_f = 3.1 \pm 0.4\ \mu m^2/s$) obtained by tracking labeled ACBP are in complete agreement with the earlier results.[5] Therefore, previous conclusions[5,6] regarding the existence of strong interactions between the solid support and both leaflets of the membrane are fully supported.

Although the lipid mobility of free-standing and supported membranes have been extensively investigated, there are only a few reports of coexisting mobile fractions in single-phase bilayers. A slow mobile fraction associated with local inhomogenieties was detected by single-molecule tracking in POPC Langmuir−Blodgett films[4] and was characterized by a diffusion constant of $0.07\ \mu m^2/s$. A minor component with $D = 0.32\ \mu m^2/s$ was obtained by a modified FRAP method applied to POPC SPBs obtained by vesicle fusion, but it was not detected by similar experiments in Langmuir−Blodgett films.[9] FCS measurements have been used to expose a slow-mobile fraction for liquid-disordered DOPC bilayers,[43] nevertheless the FRAP and FCS measurements involve averaging over many molecules, so it is challenging to use them to interpret the underlying heterogeneity in the diffusion.

To the best of our knowledge there were no previous single-molecule tracking experiments on a GUV surface. Such experiments are important because the coexistence of two mobile fractions on GUVs may not have shown up in ensemble averaged FRAP and FCS measurements. By means of the low-angle epi-illumination geometry developed for our experiments the background caused by fluorescence from the solution is considerably lower than in the usual epi-illumination scheme, furthermore the method permits tracking on the top sections of GUVs. Two fractions were not detected in our single-molecule tracking measurements and the diffusion coefficient $D = 6.9 \pm 0.3\ \mu m^2/s$ was in good agreement with the previously reported values for GUV lipid mobility using other techniques. This result unequivocally confirms the absence of a slow mobile fraction. Tracking measurements in black membranes[6] showed almost 3-fold faster diffusion than our result. This variation could either be caused by differences in tension and organization of the lipids in planar and curved GUV membranes, or become the interaction of the membranes with the support material is different in the two experiments.

The slow mobile fraction was clearly visible in the supported bilayer. Its diffusion coefficient, $D_s = 0.078 \pm 0.001\ \mu m^2/s$ was readily distinguished from D_f and is similar to that reported for Langmuir−Blodgett films on a clean glass surface.[4] This minor fraction is not associated with impurities or membrane self-defects, because it appears only upon interaction of the bilayer with the support and is not present in the parent GUV bilayer. It is known that the translational diffusion of phospholipids in supported fluid bilayers splits into two populations in the presence of surface traps.[11,18,19] The diffusion of the slow fraction in our tracking experiments is Brownian over at least a 700 ms time window and hence it cannot be attributed to restricted motion around traps at fixed locations on the glass substrate. The origin of the slow mobile fraction is not yet clear. One possibility is that it originates from the interaction of ACBP with the glass substrate. The ACBP may also have different types of interaction with the lipids of the membrane, especially at defects. The Brownian motion of the slow fraction suggests that large lipid/protein associates are moving in the membrane plane. We favor the interpretation that the bilayer adopts the roughness of the glass and acquires pore-like mobile structures on the surface of the membrane. According to theoretical[36] and experimental[37] reports on the dependence of diffusion coefficients on the size of the diffusing particle, a large number of lipids would be required to form such slowly diffusing configurations as those observed here. A configuration that incorporates a large number of lipids is a pore. The existence of pore-like traps are also a possible reason for the high affinity of the membrane for ACBP. Although approximately 1/20 of the probe molecules are associated with

(36) Saffman, P. G.; Delbrock, M. *Proc. Natl. Acad. Sci. U.S.A.* **1975**, *72*, 3111−3113.
(37) Gambin, Y.; Lopez-Esparza, R.; Reffay, M.; Sierecki, E.; Gov, N. S.; Genest, M.; Hodges, R. S.; Urbach, W. *Proc. Natl. Acad. Sci. U.S.A.* **2005**, *103*, 2098−2102.
(38) Lee, C. C.; Petersen, N. O. *Biophys. J.* **2003**, *84*, 1756−1764.
(39) Cicuta, P.; Keller, S. L.; Veatch, S. L. *J. Phys. Chem. B* **2007**, *111*, 3328−3331.
(40) Klingler, J. F.; McConnell, H. M. *J. Phys. Chem.* **1993**, *97*, 6096−6100.
(41) Doeven, M. K.; Folgering, J. H. A.; Krasnikov, V.; Geertsma, E. R.; Bogaart, G. V. d.; Poolman, B. *Biophys. J.* **2005**, *88*, 1134−1142.
(42) Hetzer, M.; Heinz, S.; Grage, S.; Bayerl, T. M. *Langmuir* **1998**, *14*, 982−984.
(43) Burns, A. R.; Frankel, D. J.; Buranday, T. *Biophys. J.* **2005**, *89*, 1081−1093.

the slow motion, the total area occupied by traps is a much smaller fraction of the bilayer area. The number of associated ACBP molecules per unit surface area is proportional to the encounter frequency, which depends on the concentration of ACBP and its solution-phase diffusion coefficient, and to the efficiency of ACBP binding on collision. It follows that ACBP must have a much higher binding affinity for the trap regions. In a pore-like structure the local curvature of the bilayer is probably similar to that at the bilayer edges where the protein associates most strongly, as shown in Figure 3 and discussed earlier. An additional detailed study would be needed to clarify the configurations corresponding to the slow mobile fraction.

Conclusions

In summary, we found that labeled ACBP proteins spontaneously attach to either GUVs or supported bilayers prior to undergoing diffusion in the bilayer plane. The diffusion constants obtained by single-molecule tracking of bound protein in the membranes are close to those reported in literature for single fluorescently labeled lipids. These results confirm that the binding of labeled proteins that are freely diffusing in the solution, can be employed along with single-molecule tracking techniques to obtain fluid properties of bilayers. A direct comparison of diffusion in a free-standing GUV bilayer and a derivative bilayer obtained by GUV rupture was made. These bilayers should only differ in the manner of their interactions with the substrate. Single-molecule tracking on flat supported bilayers and on the surface of the GUV revealed Brownian type diffusion in both cases. The diffusion in supported bilayers contained two clearly identifiable fractions, while diffusion on the surface of the GUV was homogeneous. The slowly diffusing fraction is suggested to be associated with pore-like defects arising from the roughness of the glass support.

Acknowledgment. This research was supported by The National Institutes of Health (GM72041) with instrumentation from NIH RR 01348.

Supporting Information Available: Three movies show examples of diffusion of the probes in the supported bilayer. They demonstrate fast and slow diffusing fractions and trapping events. This material is available free of charge via the Internet at http://pubs.acs.org.

LA702600W